Supporting Information

Antimony doped Tin (IV) hybrid metal halides with high efficiency tunable emission, WLED and information encryption

Wenchao Lin,[a] Qilin Wei,[a] Tao Huang,[a,] Xianfu Meng,[a] Ye Tian,[a] Hui Peng,[a,*] Bingsuo zou [a,*]

[a] State Key Laboratory of Featured Metal Materials and Life-cycle Safety for Composite Structures; School of Resources, Environments and Materials, Guangxi University, Nanning 530004, China.

* Corresponding author: Bingsuo Zou，Hui Peng

Table S1. Crystal data and structure refinement for $(C_{13}H_{30}N)_2SnCl_6$ single crystal at 296 K.

Identification code	220826H2_autored
Empirical formula	$C_{26}H_{60}Cl_6N_2Sn$
Formula weight	732.15
Temperature/K	296.15(10)
Crystal system	triclinic
Space group	P-1
a/Å	9.8400(6)
b/Å	10.8858(7)
c/Å	18.0546(9)
α/°	105.944(5)
β/°	97.101(5)
γ/°	91.271(5)
Volume/Å^3	1842.08(19)
Z	2
ρ_{calc}g/cm^3	1.320
μ/mm^{-1}	1.146
F(000)	764.0
Crystal size/mm^3	
Radiation	Mo Kα (λ = 0.71073)
2θ range for data collection	4.178 to 60.838
Index ranges	$-12 \le h \le 13$, $-9 \le k \le 15$, $-25 \le l \le 16$
Reflections collected	11745
Independent reflections	8721 [R_{int} = 0.0138, R_{sigma} = 0.0293]
Data/restraints/parameters	8721/8/362
Goodness-of-fit on F^2	1.020
Final R indexes [I>=2σ (I)]	R_1 = 0.0500, wR_2 = 0.1184
Final R indexes [all data]	R_1 = 0.0726, wR_2 = 0.1298
Largest diff. peak/hole / e Å^{-3}	0.63/-0.97

Table S2. Fractional Atomic Coordinates (×104) and Equivalent Isotropic Displacement Parameters (Å2×103) for $(C_{13}H_{30}N)_2SnCl_6$. U_{eq} is defined as 1/3 of the trace of the orthogonalised U_{IJ} tensor.

Atom	*x*	*y*	*z*	U(eq)
Sn1	2540.1(2)	3411.9(2)	7140.8(2)	50.77(10)
Cl1	721.8(10)	4645.9(11)	6695.9(7)	70.7(3)
Cl2	2267.0(16)	1929.8(13)	5846.6(8)	94.8(4)
Cl3	839.8(12)	2108.5(12)	7493.1(9)	88.6(4)
Cl4	4231.6(11)	4679.1(12)	6759.6(8)	82.3(3)
Cl5	2742.6(14)	4916.1(13)	8422.1(7)	88.3(4)
Cl6	4332.8(11)	2191.0(12)	7580.1(8)	82.4(3)
N1	7969(3)	4815(4)	8480(2)	73.4(10)
C2	9703(8)	7815(7)	8192(5)	141(3)
C3	6188(12)	8155(9)	10469(7)	214(5)
C5	9312(11)	8747(10)	7793(6)	191(4)
C7	8627(9)	2104(7)	9472(5)	144(3)
C9	7021(7)	6273(8)	9627(4)	145(3)
C10	9028(5)	5820(5)	8475(3)	88.7(15)
C14	7527(5)	4026(5)	7655(3)	87.1(15)
C18	8680(5)	3979(5)	8936(3)	87.3(15)
C19	7832(11)	1043(9)	9623(6)	186(4)
C20	6706(5)	5380(5)	8822(3)	85.4(14)
C21	5838(9)	6941(8)	9925(5)	158(3)
C22	8560(6)	6787(6)	8064(4)	106.9(19)
C24	7804(7)	2880(6)	9024(4)	106.8(18)
N2	2080(4)	7859(4)	5640(2)	75.4(10)
C1	2776(4)	5651(4)	4916(3)	71.0(11)
C4	1636(4)	6501(4)	5194(3)	71.7(11)
C6	2236(6)	8576(5)	4440(3)	94.0(16)
C8	2206(5)	4307(5)	4543(3)	83.5(13)
C11	3163(14)	8943(10)	7012(6)	114(4)
C12	2914(5)	8499(5)	5200(3)	84.1(14)
C13	2828(10)	7639(8)	6412(5)	68(2)
C15	3343(8)	9227(7)	4083(4)	125(2)
C16	810(5)	8578(6)	5811(3)	95.9(16)
C17	2741(9)	9586(7)	3432(5)	142(3)
C23	5067(15)	8470(20)	7874(11)	193(9)
C25	3639(16)	8704(15)	7812(7)	127(5)
C26	3312(6)	3410(5)	4249(4)	103.2(17)
C25A	3830(30)	8320(20)	8291(13)	164(11)
C23A	4350(20)	8510(20)	7615(9)	119(8)
C11A	2958(19)	8040(20)	7045(10)	134(9)
C13A	3209(15)	8372(17)	6357(8)	93(5)

Table S3. Anisotropic Displacement Parameters (Å^2×10^3) for $(C_{13}H_{30}N)_2SnCl_6$. The Anisotropic displacement factor exponent takes the form: $-2\pi^2[h^2a^{*2}U_{11}+2hka^*b^*U_{12}+\ldots]$.

Atom	**U$_{11}$**	**U$_{22}$**	**U$_{33}$**	**U$_{23}$**	**U$_{13}$**	**U$_{12}$**
Sn1	42.85(14)	45.62(14)	62.38(17)	15.71(11)	0.79(10)	-0.89(9)
Cl1	57.4(5)	76.2(7)	79.9(7)	28.5(5)	-1.9(5)	14.9(5)
Cl2	108.8(10)	74.4(7)	81.7(8)	-7.7(6)	5.6(7)	5.9(7)
Cl3	63.6(6)	77.9(7)	135.2(11)	42.7(7)	27.4(7)	-6.3(5)
Cl4	61.0(6)	83.4(7)	118.4(9)	57.0(7)	9.2(6)	-6.6(5)
Cl5	87.8(8)	91.1(8)	68.0(7)	0.0(6)	-7.9(6)	8.6(7)
Cl6	59.3(6)	78.4(7)	126.0(10)	55.8(7)	10.9(6)	15.6(5)
N1	50.2(18)	94(3)	63(2)	3.4(19)	0.5(15)	-0.3(18)
C2	146(7)	116(6)	170(7)	48(5)	40(6)	-13(5)
C3	241(13)	130(8)	249(12)	0(8)	73(10)	10(8)
C5	234(12)	176(9)	198(10)	81(8)	100(9)	15(8)
C7	152(7)	115(6)	151(7)	41(5)	-34(5)	-17(5)
C9	110(5)	183(8)	102(5)	-33(5)	31(4)	17(5)
C10	62(3)	94(4)	98(4)	8(3)	10(3)	-8(2)
C14	64(3)	110(4)	68(3)	-2(3)	-1(2)	-3(3)
C18	69(3)	98(4)	78(3)	7(3)	-11(2)	4(3)
C19	235(12)	164(9)	169(8)	80(7)	-4(8)	7(8)
C20	61(3)	104(4)	88(3)	16(3)	19(2)	12(2)
C21	153(7)	159(7)	125(6)	-35(5)	48(5)	20(6)
C22	95(4)	113(5)	113(4)	22(4)	37(4)	3(4)
C24	103(4)	123(5)	91(4)	32(4)	-6(3)	-3(4)
N2	61(2)	98(3)	60(2)	12(2)	2.6(16)	14.9(19)
C1	61(2)	78(3)	82(3)	32(2)	13(2)	6(2)
C4	61(2)	86(3)	74(3)	33(2)	8(2)	5(2)
C6	110(4)	74(3)	106(4)	26(3)	39(3)	7(3)
C8	67(3)	79(3)	113(4)	43(3)	7(3)	5(2)

C11	179(12)	72(6)	70(6)	5(5)	-31(6)	18(7)
C12	73(3)	67(3)	97(4)	0(3)	11(3)	-6(2)
C13	88(5)	55(4)	57(5)	23(4)	-10(4)	-5(4)
C15	153(7)	117(5)	111(5)	38(4)	25(5)	9(5)
C16	85(3)	120(4)	86(3)	27(3)	21(3)	34(3)
C17	167(8)	100(5)	166(7)	39(5)	53(6)	-1(5)
C23	133(14)	260(20)	192(19)	109(17)	-37(13)	-31(15)
C25	175(17)	120(10)	64(9)	0(7)	-9(9)	5(10)
C26	84(4)	85(4)	138(5)	26(3)	17(3)	14(3)
C25A	210(30)	141(18)	135(19)	54(15)	-40(18)	-42(17)
C23A	106(16)	176(19)	48(9)	-13(10)	-2(9)	47(15)
C11A	180(20)	151(19)	82(13)	49(13)	24(12)	86(17)
C13A	85(9)	83(11)	94(11)	5(9)	-8(7)	-1(8)

Table S4. Bond Lengths for $(C_{13}H_{30}N)_2SnCl_6$.

Atom	**Atom**	**Length/Å**	**Atom**	**Atom**	**Length/Å**
Sn1	Cl1	2.4485(10)	C18	C24	1.514(8)
Sn1	Cl2	2.4269(12)	N2	C4	1.502(6)
Sn1	Cl3	2.4229(11)	N2	C12	1.493(6)
Sn1	Cl4	2.4187(11)	N2	C13	1.575(8)
Sn1	Cl5	2.4214(12)	N2	C16	1.509(6)
Sn1	Cl6	2.4175(10)	N2	C13A	1.563(14)
N1	C10	1.496(6)	C1	C4	1.516(6)
N1	C14	1.506(5)	C1	C8	1.496(6)

N1	C18	1.515(6)	C6	C12	1.474(7)
N1	C20	1.523(6)	C6	C15	1.580(9)
C2	C5	1.431(11)	C8	C26	1.525(7)
C2	C22	1.520(9)	C11	C13	1.531(13)
C3	C21	1.419(11)	C11	C25	1.555(11)
C7	C19	1.485(11)	C15	C17	1.405(10)
C7	C24	1.506(9)	C23	C25	1.430(12)
C9	C20	1.501(8)	C25A	C23A	1.443(17)
C9	C21	1.466(9)	C23A	C11A	1.590(17)
C10	C22	1.496(8)	C11A	C13A	1.432(17)

Table S5. Bond Angles for $(C_{13}H_{30}N)_2SnCl_6$.

Atom	Atom	Atom	Angle/˚	Atom	Atom	Atom	Angle/˚
Cl2	Sn1	Cl1	89.06(5)	C9	C20	N1	113.8(4)
Cl3	Sn1	Cl1	90.03(4)	C3	C21	C9	113.9(8)
Cl3	Sn1	Cl2	89.09(5)	C10	C22	C2	109.3(6)
Cl4	Sn1	Cl1	89.96(4)	C7	C24	C18	111.0(5)
Cl4	Sn1	Cl2	89.60(5)	C4	N2	C13	99.9(4)
Cl4	Sn1	Cl3	178.69(5)	C4	N2	C16	108.0(4)
Cl4	Sn1	Cl5	90.92(5)	C4	N2	C13A	129.1(7)
Cl5	Sn1	Cl1	89.20(4)	C12	N2	C4	112.2(3)
Cl5	Sn1	Cl2	178.18(5)	C12	N2	C13	117.0(5)
Cl5	Sn1	Cl3	90.39(5)	C12	N2	C16	109.8(4)
Cl6	Sn1	Cl1	179.91(4)	C12	N2	C13A	87.7(7)

Cl6	Sn1	Cl2	90.91(5)	C16	N2	C13	109.3(5)
Cl6	Sn1	Cl3	89.89(4)	C16	N2	C13A	107.8(7)
Cl6	Sn1	Cl4	90.13(4)	C8	C1	C4	110.0(4)
Cl6	Sn1	Cl5	90.83(5)	N2	C4	C1	115.7(4)
C10	N1	C14	108.4(4)	C12	C6	C15	105.9(5)
C10	N1	C18	106.0(4)	C1	C8	C26	112.1(4)
C10	N1	C20	112.7(4)	C13	C11	C25	107.8(10)
C14	N1	C18	109.2(4)	C6	C12	N2	116.0(4)
C14	N1	C20	108.4(3)	C11	C13	N2	108.5(7)
C18	N1	C20	112.1(4)	C17	C15	C6	111.1(7)
C5	C2	C22	111.2(8)	C23	C25	C11	109.7(13)
C19	C7	C24	114.8(7)	C25A	C23A	C11A	95.1(18)
C21	C9	C20	114.2(6)	C13A	C11A	C23A	103.2(15)
C22	C10	N1	116.1(4)	C11A	C13A	N2	115.2(15)
C24	C18	N1	115.9(4)				

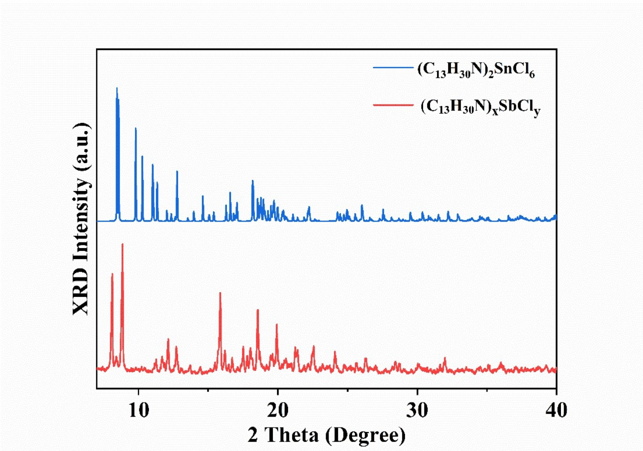

Figure S1. The simulated and experimental powder X-ray diffraction patterns of $(C_{13}H_{30}N)_2SnCl_6$ and $(C_{13}H_{30}N)_xSbCl_y$.

Table S6. Elements content of $(C_{13}H_{30}N)_2SnCl_6$:20%Sb from the quantitative analysis of EDS data.

Sample	Sn (At %)	Sb (At %)	Cl (At %)	Sb/(Sn+Sb)
$(C_{13}H_{30}N)_2SnCl_6$:20%Sb	13.44	1.80	84.77	11.81%

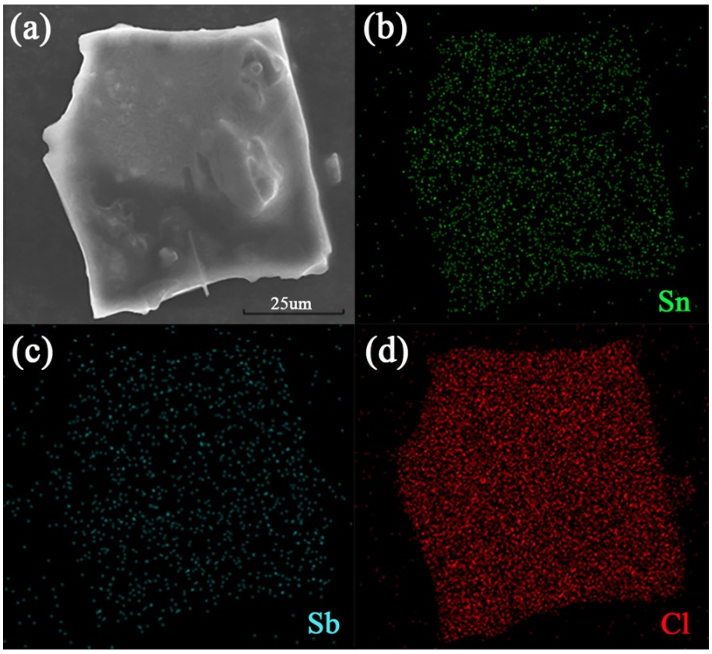

Figure S2. SEM image of $(C_{13}H_{30}N)_2SnCl_6$:20%Sb (a) and corresponding EDS mappings of Sn(b), Sb(c) and Cl(d) elements.

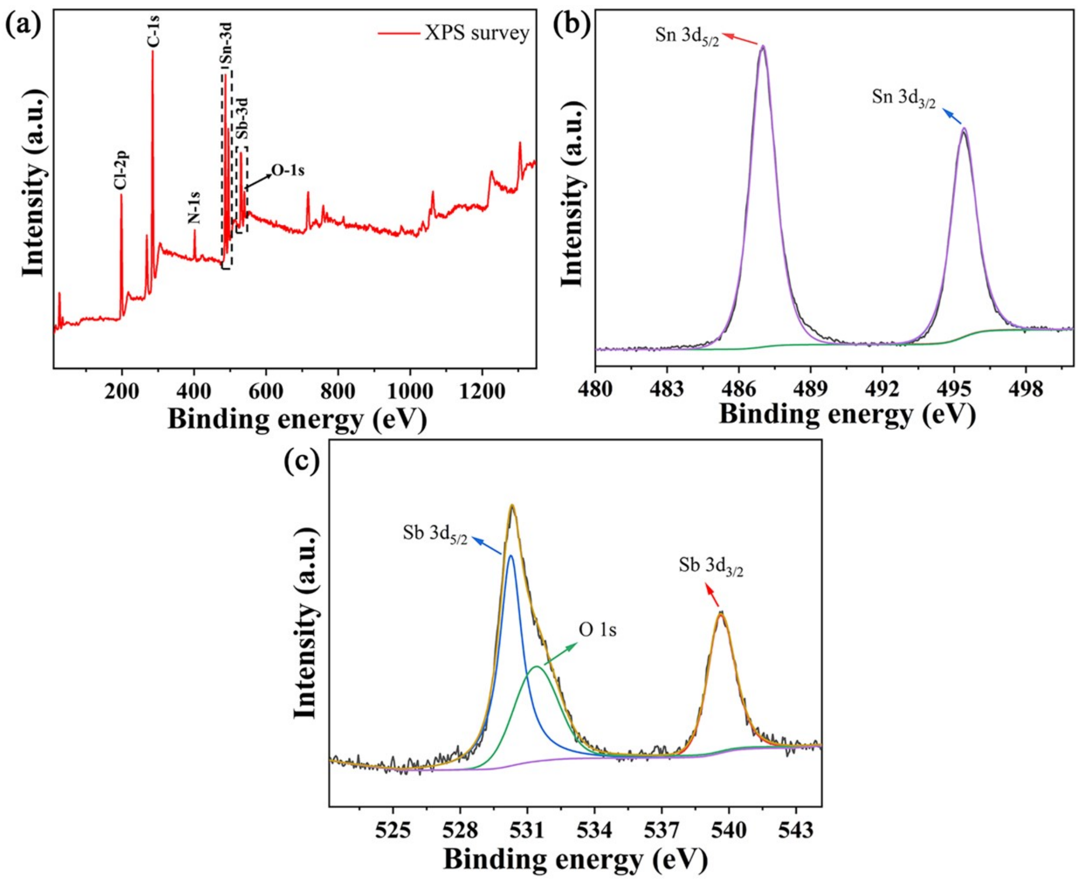

Figure S3. (a) XPS spectrum for the $(C_{13}H_{30}N)_2SnCl_6$:20%Sb powder, (b) Sn 3d XPS spectrum, (c) Sb 3d XPS spectrum.

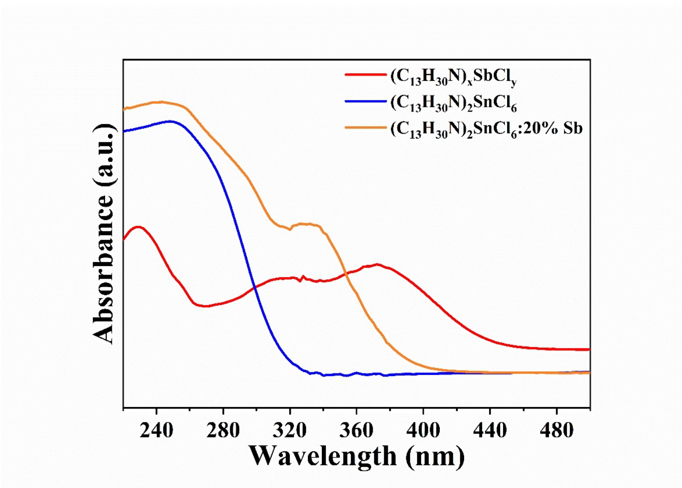

Figure S4. Absorption spectra of $(C_{13}H_{30}N)_xSnCl_y$, $(C_{13}H_{30}N)_2SnCl_6$ and $(C_{13}H_{30}N)_2SnCl_6$: 20%Sb.

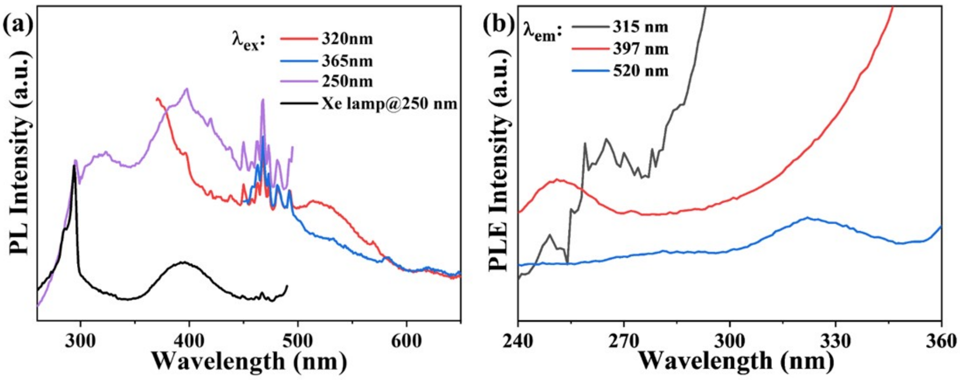

Figure S5. PL (a) and PLE (b) spectra of $(C_{13}H_{30}N)_2SnCl_6$ monitored at different wavelengths.

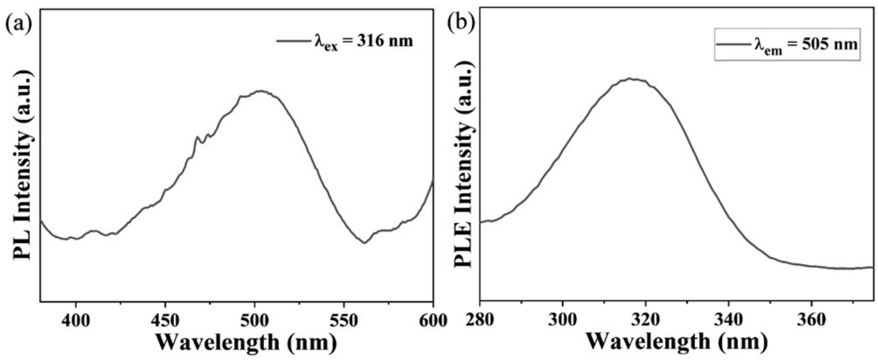

Figure S6. PL (a) and PLE (b) spectra of $C_{13}H_{30}NCl$.

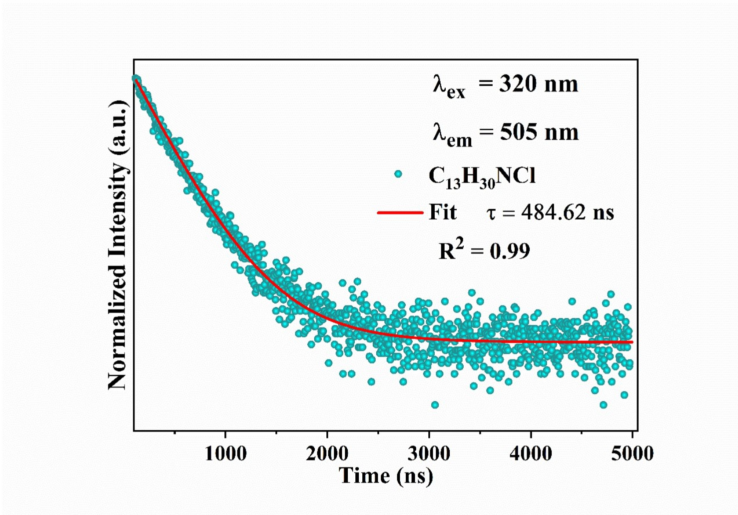

Figure S7. The lifetime decay curves of the $C_{13}H_{30}NCl$ for the 505 nm emission (λ_{ex} = 320 nm).

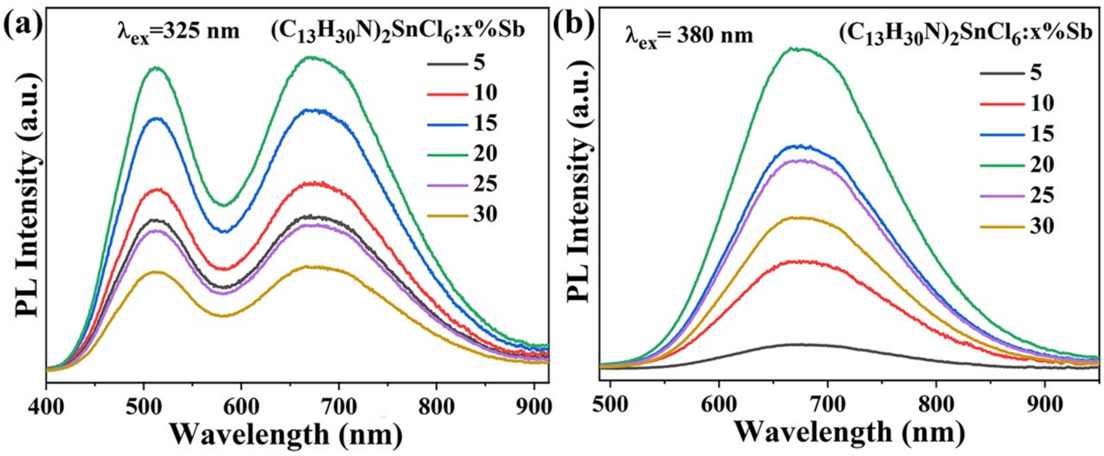

Figure S8. PL spectra of $(C_{13}H_{30}N)_2SnCl_6$:x%Sb under different excitations.

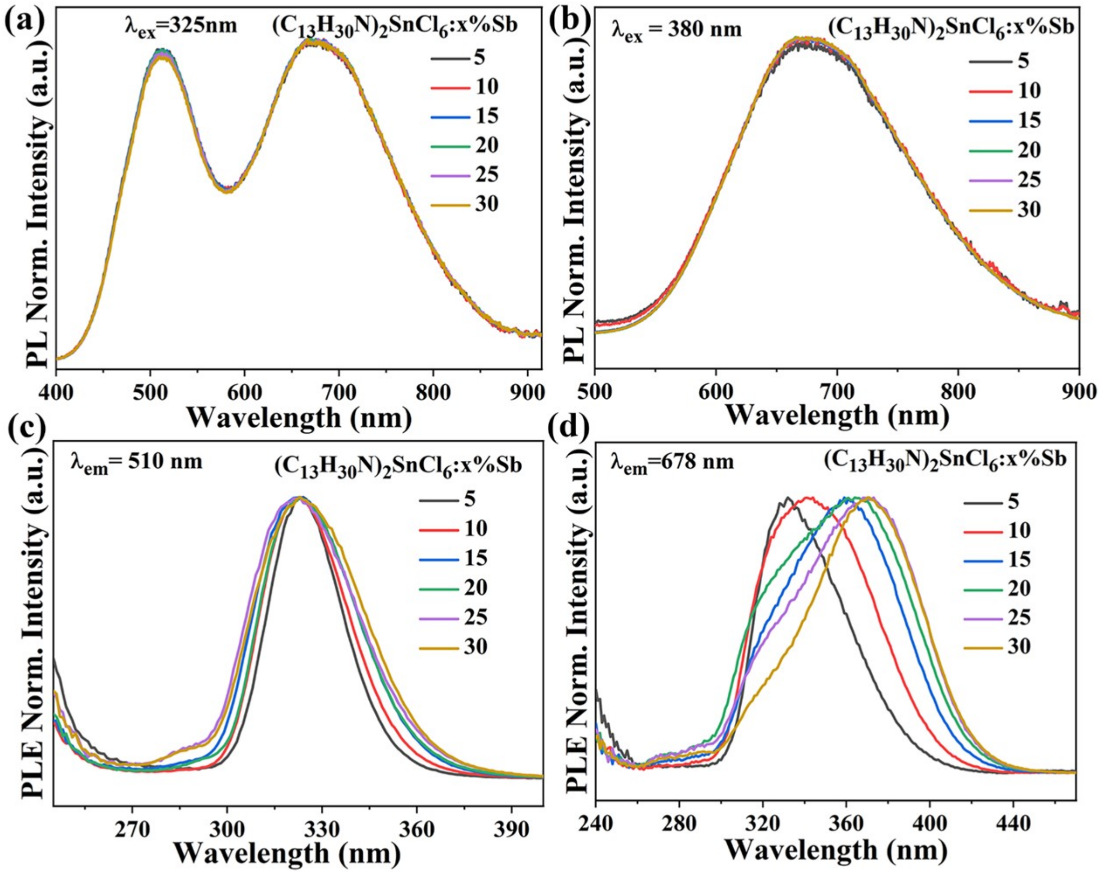

Figure S9. Normalized PL and PLE spectra monitored at different wavelengths of $(C_{13}H_{30}N)_2SnCl_6$:x%Sb.

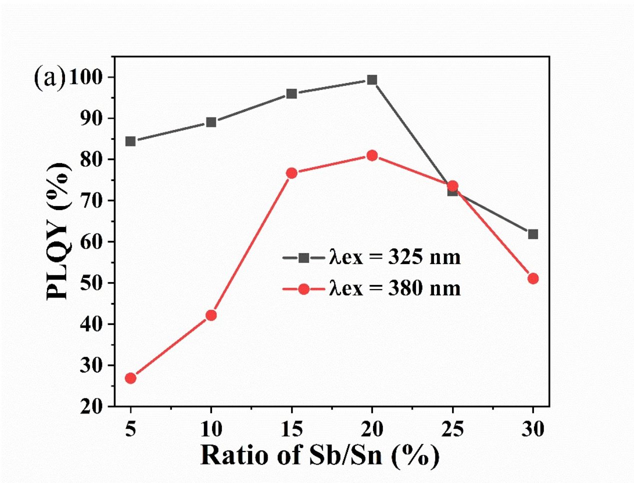

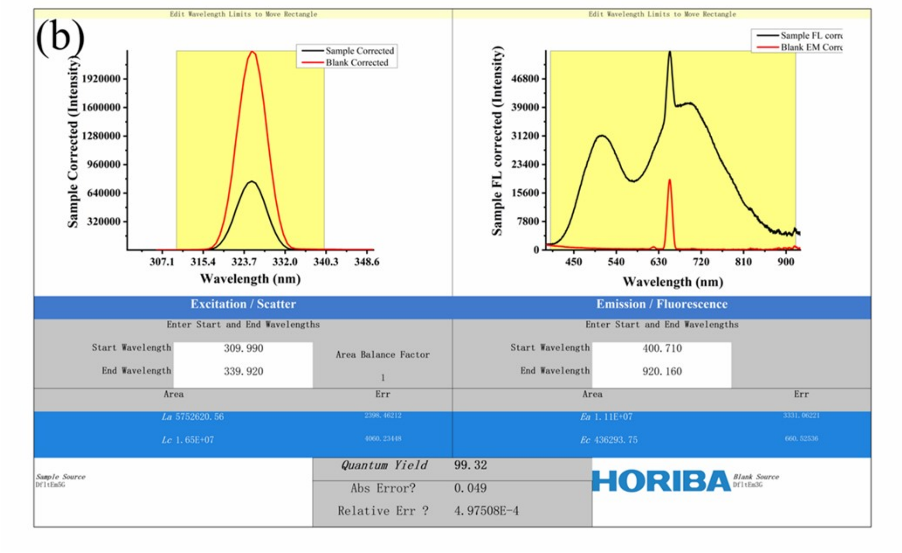

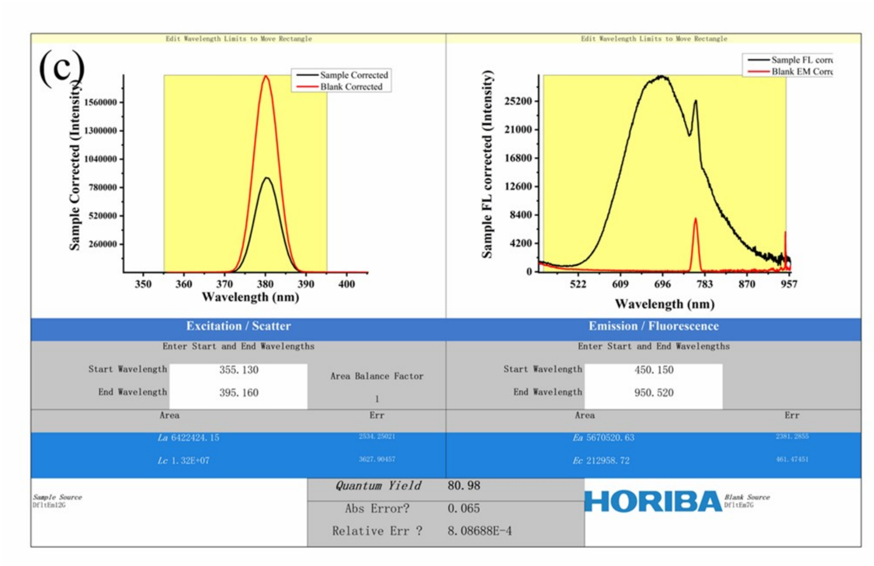

Figure S10. (a) Plot of PLQY with Sb/Sn ratio, best PLQY under 325nm excitation (b) (Sb/Sn = 20%) and 380nm excitation (c) (Sb/Sn = 20%).

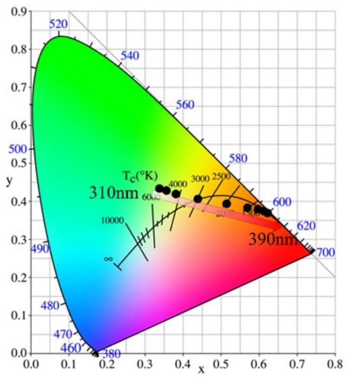

Figure S11. CIE coordinates of $(C_{13}H_{30}N)_2SnCl_6$:20%Sb in the 1931 color space chromaticity diagram under different excitation wavelengths.

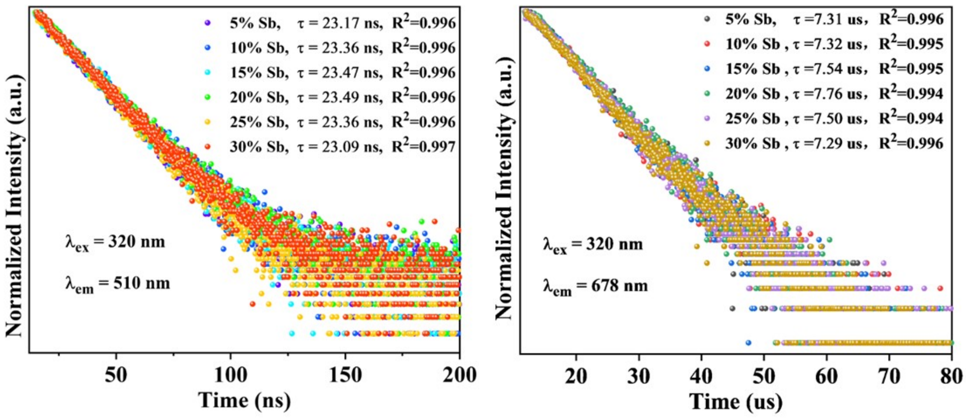

Figure S12. Lifetime decay curve of $(C_{13}H_{30}N)_2SnCl_6$: x% Sb under different emission centers.

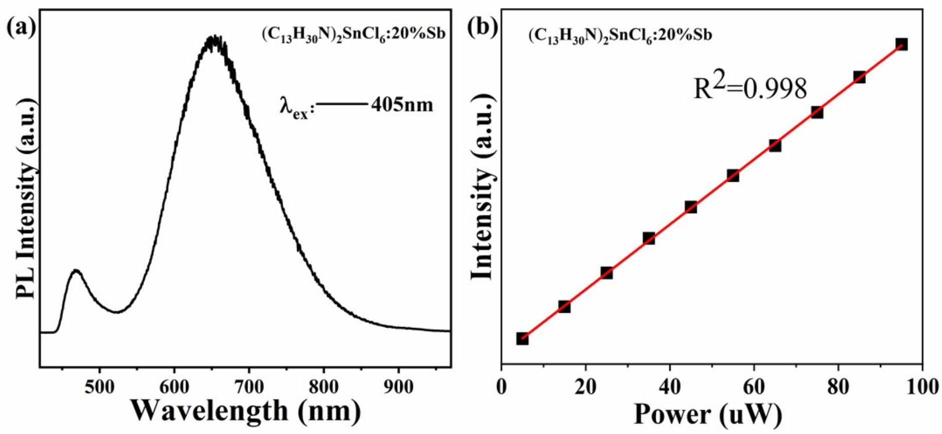

Figure S13. (a) PL spectra of $(C_{13}H_{30}N)_2SnCl_6$:20%Sb monitored at 405nm laser**.** (b) The relationship between emission intensity and excitation power of $(C_{13}H_{30}N)_2SnCl_6$: 20% Sb was measured using a 405nm laser. The linear fit result has a high R^2 value of 0.998.

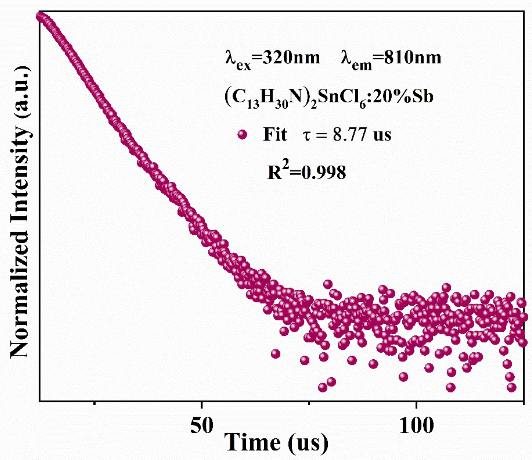

Figure S14. Lifetime decay curve of $(C_{13}H_{30}N)_2SnCl_6$: 20% Sb at 810 nm.

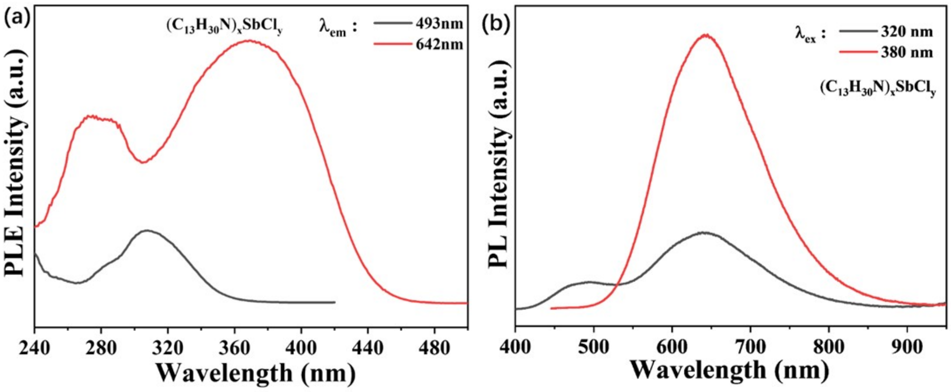

Figure S15. PLE (a) and PL (b) spectrum of $(C_{13}H_{30}N)_xSbCl_y$.

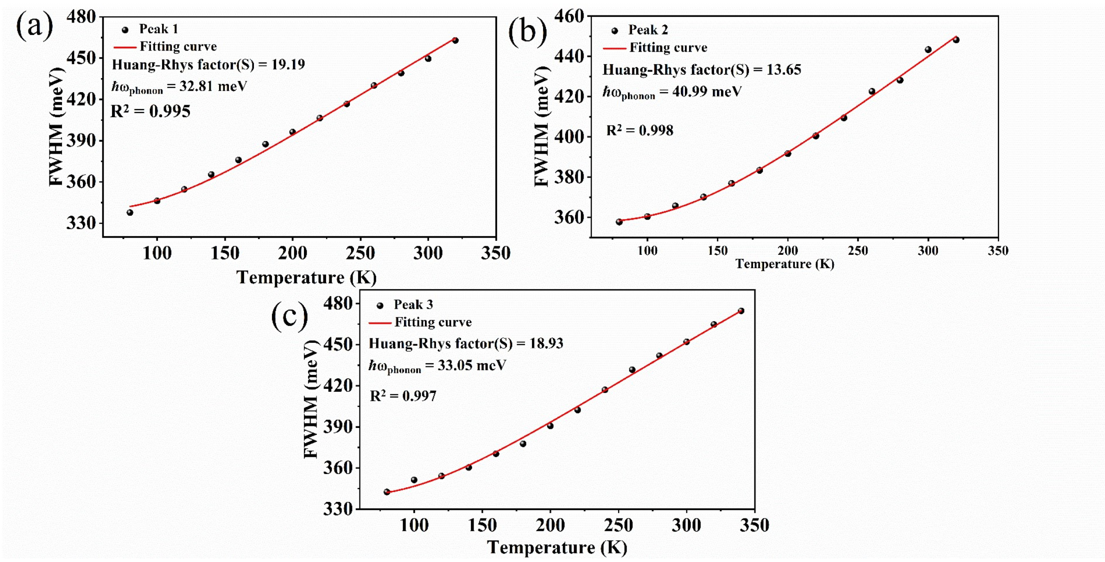

Figure S16. The fitting results of full width at half maximum (FWHM) as a function of temperature for (a)Peak 1, (b)Peak 2 and (c)Peak 3.

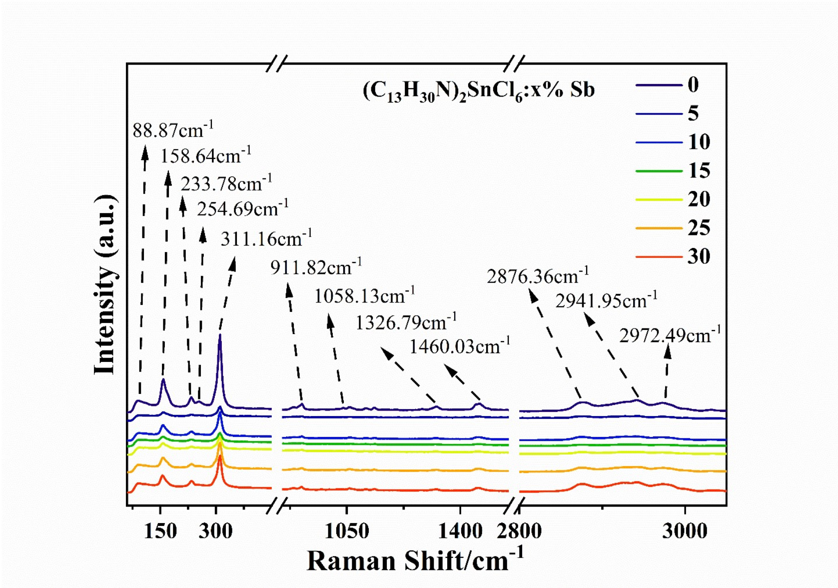

Figure S17. Raman spectrum (60-3050 cm^{-1}) excited by 633 nm laser.

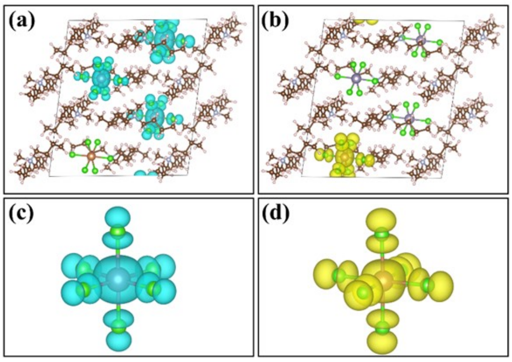

Figure S18. Partial charge densities of (a) CBM and (b) VBM in Sb^{3+}-doped $(C_{13}H_{30}N)_2SnCl_6$ with $[SbCl_5]^{3-}$ and $[SnCl_6]^{2-}$ units. For clarity, (c) single $[SnCl_6]^{2-}$ and (d) $[SbCl_6]^{3-}$ units are shown.

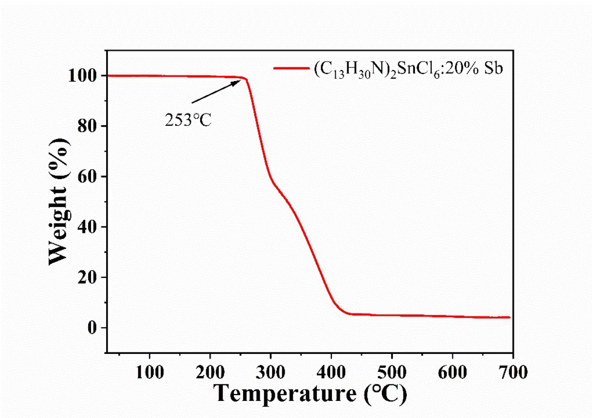

Figure S19. Thermogravimetric analysis (TGA) curves of $(C_{13}H_{30}N)_2SnCl_6$: 20% Sb.

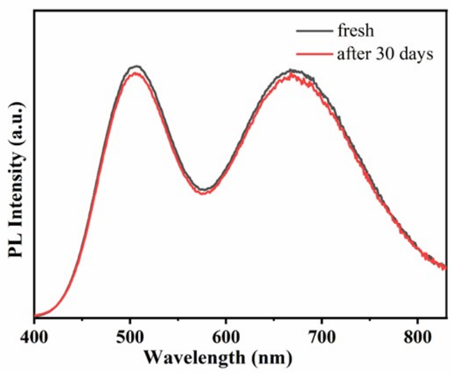

Figure S20. Emission intensity comparison of $(C_{13}H_{30}N)_2SnCl_6$: 20% Sb powder before and after exposure to air for 30 days.

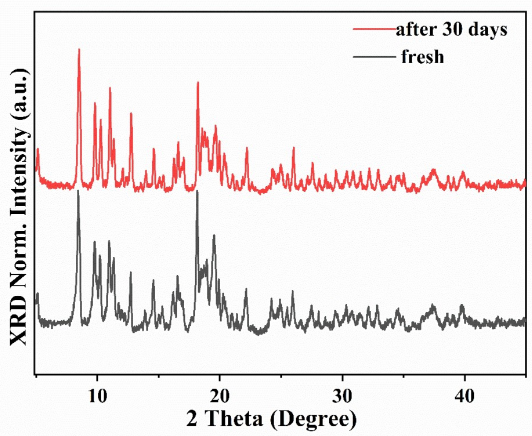

Figure S21. XRD comparison of $(C_{13}H_{30}N)_2SnCl_6$: 20% Sb powder before and after exposure to air for 30 days.

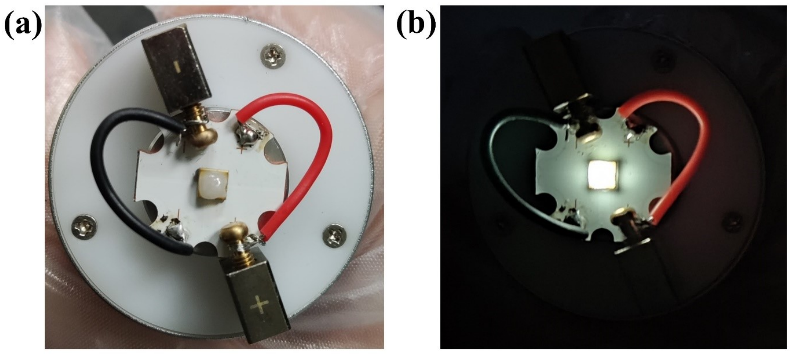

Figure S22. Photographs of WLED devices under daylight and 90mA drive current.

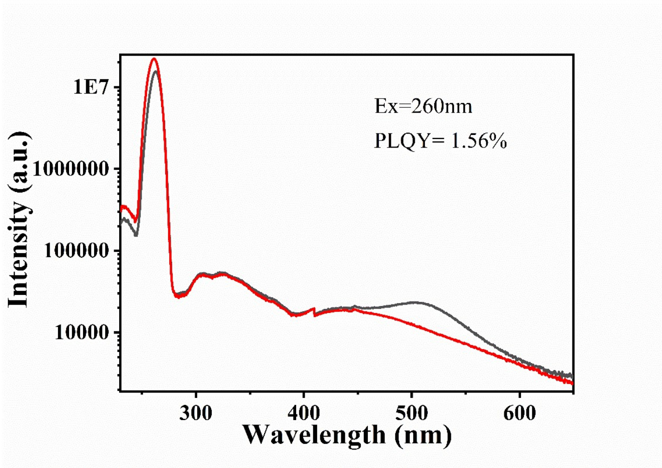

Figure S23. The PLQY of $(C_{13}H_{30}N)_2SnCl_6$ at 260nm.

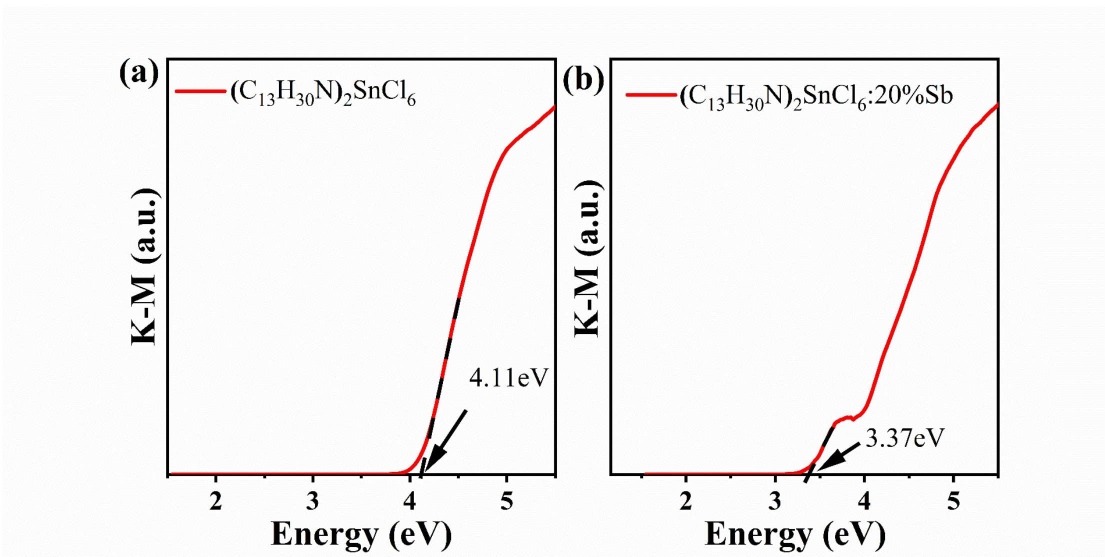

Figure S24. Experimental band gap values of $(C_{13}H_{30}N)_2SnCl_6$ (a) and $(C_{13}H_{30}N)_2SnCl_6$:20%Sb (b).

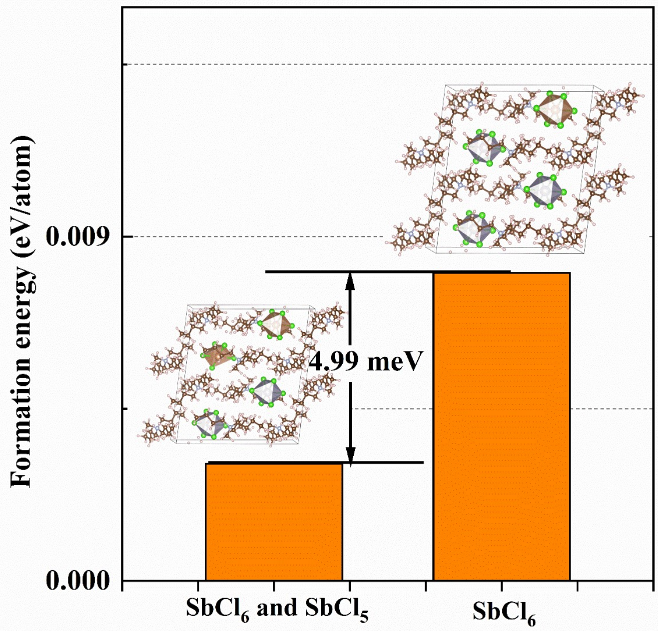

Figure S25. Formation energy comparison diagram of only $SbCl_6$ clusters and simultaneous formation of $SbCl_5$ and $SbCl_6$ clusters in $(C_{13}H_{30}N)_2SnCl_6$.

Table S7. Comparison of this work with already reported PLQY and CRI properties of tin (IV) halides.

Chemical formula	Highest CRI	Highest PLQY (%)	CIE of the sample	CIE of LED devices	Stokes shift (nm)	FWHM (nm)	PL Peak position (nm)	Ref.
$(C_{13}H_{30}N)_2SnCl_6$: Sb	96.7	99.32	(0.36,0.42)	(0.346,0.38)	185/298	~/171	510/678	this work
$(C_9H_8N)_2SnCl_6$	N/A	41	(0.16,0.12)	N/A	144	86	433	1
$(4\text{-}APEA)_2SnBr_6$	N/A	27	(0.44,0.52)	N/A	222	111	566	2
$C_{16}H_{22}Cl_6F_2N_2Sn$/ $C_{16}H_{22}Br_6F_2N_2Sn$	N/A	N/A	N/A	N/A	N/A	N/A	N/A	3
$(C_6N_2H_{16}Cl)_2SnCl_6$	N/A	8.1	(0.21,0.24)	N/A	75	125	450	4
$(C_9H_{14}N)_2[SnCl_6]$	N/A	N/A	N/A	N/A	114	N/A	407	5
$(C_5H_{14}N_2)_2[SnCl_6]_2\cdot 5H_2O$	N/A	N/A	N/A	N/A	N/A	N/A	600	6
$(C_5N_2H_{14})SnCl_6$	97	N/A	(0.39,0.43)/ (0.45,0.43)	N/A	367/380	203/254	570/680	7
$(Ph_3S)_2SnCl_6$	N/A	17.5	N/A	N/A	27/150	N/A	382/505	8
$(Ph_3S)_2Sn_{1-x}Te_xCl_6$	N/A	2.5	N/A	N/A	240/165	N/A	595/520	8
$(NH_4)_2SnCl_6$: Te	88	83.51	N/A	(0.31,0.29)	200	127	590	9
$(C_8H_{22}N_2Cl)_2SnCl_6$: Sb	N/A	41.76	N/A	N/A	350	178	690	10
$(C_{10}H_{16}N_2)SnCl_6$:Sb	84	77	N/A	(0.32,0.34)	N/A	N/A	500/600	11
$(NH_4)_2SnCl_6$:Sb	N/A	58	N/A	N/A	200/374	N/A	590/734	12
Cs_2SnCl_6: Sb	81	37	(0.55,0.45)	(0.30,0.37)	101	237	605	13
Cs_2SnBr_6	84.09	31	N/A	(0.52,0.41)	255	121	600	14
Cs_2SnCl_6: Bi	N/A	78.9	N/A	(0.36, 0.37)	95	66	455	15
$Cs_2Sn_{1-x}Te_xCl_6$	N/A	95.4	N/A	N/A	120	>100	580	16
Rb_2SnCl_6:Bi	N/A	21	N/A	N/A	70	65	426	17
$Cs_2Pt_xSn_{1-x}Cl_6$	N/A	22	N/A	N/A	180	110	640/433	18
Cs_2SnCl_6:Te	N/A	42.3	N/A	N/A	188	N/A	573	19

references

1. S. Zhou, L. Zhou, Y. Chen, W. Shen, M. Li and R. He, *J. Phys. Chem. Lett.*, 2022, **13**, 8717-8724.
2. Q. Chen, M. Zhang, F. Dai, L. Zhao, S. Liu, H. Zhao, H. Zhou, L. Teng, W. Xu, L. Wang and J. Xing, *Adv. Opt. Mater.*, 2022, **11**, 2202475.

3. X. You, J. Yao and Z. Wei, *Dalton Trans.*, 2020, **49**, 7252-7257.
4. G. Song, M. Li, Y. Yang, F. Liang, Q. Huang, X. Liu, P. Gong, Z. Xia and Z. Lin, *J. Phys. Chem. Lett.*, 2020, **11**, 1808-1813.
5. I. Feddaoui, M. S. M. Abdelbaky, S. García-Granda, K. Essalah, C. Ben Nasr and M. L. Mrad, *J. Mol. Struct.*, 2019, **1186**, 31-38.
6. S. BelhajSalah, M. S. M. Abdelbaky, S. García-Granda, K. Essalah, C. Ben Nasr and M. L. Mrad, *Solid State Sci.*, 2018, **86**, 77-85.
7. G. Song, Z. Li, P. Gong, R. J. Xie and Z. Lin, *Adv. Opt. Mater.*, 2021, **9**, 2002246.
8. Z. Luo, Y. Liu, Y. Liu, C. Li, Y. Li, Q. Li, Y. Wei, L. Zhang, B. Xu, X. Chang and Z. Quan, *Adv. Mater.*, 2022, **34**, 2200607.
9. Z. Li, C. Zhang, B. Li, C. Lin, Y. Li, L. Wang and R.-J. Xie, *Chem. Eng. J.*, 2021, **420**, 129740.
10. L. Zhou, L. Zhang, H. Li, W. Shen, M. Li and R. He, *Adv. Funct. Mater.*, 2021, **31**, 2108561.
11. G. Zhang, P. Dang, H. Xiao, H. Lian, S. Liang, L. Yang, Z. Cheng, G. Li and J. Lin, *Adv. Opt. Mater.*, 2021, **9**, 2101637.
12. H. Lin, Q. Wei, B. Ke, W. Lin, H. Zhao and B. Zou, *J. Phys. Chem. Lett.*, 2023, **14**, 1460-1469.
13. J. Li, Z. Tan, M. Hu, C. Chen, J. Luo, S. Li, L. Gao, Z. Xiao, G. Niu and J. Tang, *Front. Optoelectron.*, 2019, **12**, 352-364.
14. C.-F. Lai, Y.-C. Chang and Y.-C. Tien, *ACS Appl. Nano Mater.*, 2021, **4**, 1924-1931.
15. Z. Tan, J. Li, C. Zhang, Z. Li, Q. Hu, Z. Xiao, T. Kamiya, H. Hosono, G. Niu, E. Lifshitz, Y. Cheng and J. Tang, *Adv. Funct. Mater.*, 2018, **28**, 1801131.
16. Z. Tan, Y. Chu, J. Chen, J. Li, G. Ji, G. Niu, L. Gao, Z. Xiao and J. Tang, *Adv. Mater.*, 2020, **32**, 2002443.
17. S. A. Qamar, T.-W. Lin, Y.-T. Tsai and C. C. Lin, *ACS Appl. Nano Mater.*, 2022, **5**, 7580-7587.
18. H. Yin, J. Chen, P. Guan, D. Zheng, Q. Kong, S. Yang, P. Zhou, B. Yang, T. Pullerits and K. Han, *Angew. Chem., Int. Ed.*, 2021, **60**, 22693-22699.
19. R. Zeng, K. Bai, Q. Wei, T. Chang, J. Yan, B. Ke, J. Huang, L. Wang, W. Zhou, S. Cao, J. Zhao and B. Zou, *Nano Res.*, 2020, **14**, 1551-1558.